

Many-body interference at the onset of chaos

Eric Brunner,^{1,2,*} Lukas Pausch,^{1,2,†} Edoardo G. Carnio,^{1,2}
Gabriel Dufour,^{1,2} Alberto Rodríguez,³ and Andreas Buchleitner^{1,2}

¹*Physikalisches Institut, Albert-Ludwigs-Universität Freiburg, Hermann-Herder-Straße 3, 79104, Freiburg, Germany*

²*EUCOR Centre for Quantum Science and Quantum Computing,*

Albert-Ludwigs-Universität Freiburg, Hermann-Herder-Straße 3, 79104, Freiburg, Germany

³*Departamento de Física Fundamental, Universidad de Salamanca, E-37008 Salamanca, Spain*

(Dated: Friday 16th September, 2022)

We monitor the signature of many-body interference across dynamical regimes of the Bose-Hubbard model. Decreasing the particles' distinguishability increases the temporal fluctuations of few-body observables, with a dramatic amplification at the onset of quantum chaos. By resolving the exchange symmetries of partially distinguishable particles, we explain this amplification as the fingerprint of a generic initial state's coherences in the eigenbasis. In the domain of fully developed quantum chaos, ergodic delocalization of the eigenstates suppresses this fingerprint.

Interacting many-particle dynamics may be considered *the* most plausible origin of instabilities, chaos and complexity, from astronomical [1, 2] to microscopic [3] scales. Due to the rapid growth of phase space with the particle number, together with its progressively more intricate topology, deterministic descriptions quickly hit the ceiling, enforcing thermodynamic or statistical, yet not less reliable descriptions. Some type of coarse graining, implicit to such approaches, allows classifications of dynamical behavior—e.g., as integrable, mixed regular-chaotic, fully chaotic, or (non-) Markovian—associated with *universal* characteristics which are formalized, e.g., in the theories of phase transitions [4, 5], random matrices (RMT) [6], or open quantum systems [7–9]. It is the universal character of these features which allows robust predictions, since full resolution of complex dynamics is prohibitive, by their very nature.

On the quantum level, robust features are in such scenarios essentially controlled by spectral densities and statistics, the localization properties of eigen- and initial states, the phase space dimension, and the time scales over which to make predictions. This is the unifying view of quantum chaos [10], which has proven enormously versatile an approach to analyze complex quantum systems—including paradigmatic many-particle scenarios in nuclear [11, 12] and atomic physics [13–15], as well as in cold matter [16–19] and black hole [20] contexts. On this level of description, the specific many-particle nature of the underlying Hamiltonian does not appear as an essential ingredient anymore, since all the features of complex dynamics can be observed on the level of single particle dynamics [10, 21] (provided the phase space dimension is large enough—such that tori are not isolating anymore [22]).

Yet, quantum systems composed of identical particles undeniably exhibit properties which fundamentally distinguish them from classical many- and single-particle systems, hardwired in exchange symmetries [23, 24], and generating many-body interference (MBI) phenomena [25–38], thus with potentially dramatic dynamical rel-

evance. Furthermore, modern experiments [19, 39–47] allow to control external and internal degrees of freedom (dof) of many-particle quantum systems, such that physically identical particles may be equipped with continuously tunable degrees of partial distinguishability (PD), from fully indistinguishable to perfectly distinguishable, to ultimately control the impact of MBI on the many-body dynamics. While, traditionally, the RMT approach deliberately divides out such symmetry-induced properties [6, 10] (see, however, [48]), it is therefore clear that MBI is one of those robust features of many-body quantum systems which need to be accounted for in any complete theory of complex quantum systems. *Where in a many-body quantum system's spectral and eigenstate structure is MBI encoded, and how can we distill its impact on observable dynamical properties?* This is our guiding question hereafter.

We consider the one-dimensional Bose-Hubbard model [40, 49–52] of PD particles with hard-wall boundary conditions,

$$H = -J \sum_{\langle i,j \rangle} \sum_{\sigma=1}^s a_{i\sigma}^\dagger a_{j\sigma} + \frac{U}{2} \sum_{i=1}^L N_i(N_i - 1), \quad (1)$$

experimentally realizable with ultracold atoms in optical lattices [19, 39–47]. The first index of the creation and annihilation operators $a_{i\sigma}^\dagger, a_{j\sigma}$ refers to the L Wannier orbitals of the lattice, which span the *external* single-particle Hilbert space \mathcal{H}_{ext} . The second index σ refers to a basis of the s -dimensional *internal* single-particle Hilbert space, describing, e.g., the electronic state of an atom loaded into an optical lattice. The operator $N_i = \sum_{\sigma=1}^s a_{i\sigma}^\dagger a_{i\sigma}$ counts the number of particles on lattice site i , irrespective of their internal state. We keep the total particle number $N = \sum_{i=1}^L N_i$ fixed. The two terms in H describe nearest-neighbor, $\langle i, j \rangle$, tunneling and on-site interaction of the particles, both of which act exclusively on the external dof, while the internal dof remain static. For indistinguishable bosons, depending on the relative contribution of both terms in (1), a quan-

tum chaotic region has been identified from spectral and eigenstate statistics [19, 46, 47, 53–61], whose existence we will here establish also for PD particles, as an important corollary of our subsequent analysis.

Alike the Hamiltonian, observables are assumed to exclusively act on external dof, such that we can consider their restriction to $\mathcal{H}_{\text{ext}}^{\otimes N}$ and trace out the internal dof from the full system state ϱ to obtain $\rho = \text{tr}_{\text{int}} \varrho$ [35, 36, 62]. Partial distinguishability of the particles results in entanglement between their external and internal dof [35, 36], which manifests in a purity $\gamma = \text{tr} \rho^2 < 1$ of the external state, while external and internal states of indistinguishable particles are uncorrelated, such that $\gamma = 1$ [35, 62].

Of experimental interest are few-particle observables, e.g., low-order density correlations $O = N_i N_j$. Formally, these are given by products of k creation and k annihilation operators [32, 34], $k \ll N$, such that they only access the marginal information inscribed into the time-evolved k -particle (k P) reduced state [36, 62]. The system's dynamical equilibration, on asymptotic time scales, is captured by the temporal variance of the associated expectation values $\langle O(t) \rangle$:

$$\text{Var}_t[O] = \overline{\langle O(t) \rangle^2} - \overline{\langle O(t) \rangle}^2, \quad (2)$$

where $\overline{\dots}$ indicates the average over the positive time axis [63].

To formulate general statements, independent of the specific choice of observable, we consider an unbiased average (indicated by $\widehat{\dots}$) over an orthonormal basis \mathcal{B} of the (finite-dimensional) Hilbert space of external k P observables [64],

$$v := \widehat{\text{Var}_t[O]} = \sum_{o \in \mathcal{B}} \text{Var}_t[o], \quad (3)$$

This quantity is shown, for $k = 2$, in Fig. 1 (top panel), for the dynamics generated by (1), with $N = L = 6$, initially one particle per external mode, versus the control parameter J/U . A variable level of PD, as measured by γ , is obtained by random generation [63] of the internal state $|\phi_i\rangle = \sum_{\sigma} \phi_{i\sigma} |\sigma\rangle$ of the particle prepared in mode i , $\forall i$, such as to smoothly cover the entire range $\gamma \in [1/N!; 1]$.

We observe that, for all J/U , v monotonically increases with γ . Moreover, v exhibits a maximum v_{max} at $J/U \simeq 0.23$, and then decreases to a plateau value v_{∞} with increasing J/U . The peak is located at the transition to the (grey shaded) parameter range where (1) exhibits fully developed quantum chaos as identified by the ergodicity properties of its eigenstates (see discussion of Fig. 2(a) below). Both v_{∞} and the enhancement $q = v_{\text{max}}/v_{\infty}$ of the fluctuations at the peak increase monotonically with γ , as shown in the inset. In particular, q steeply increases at small γ , when MBI starts to kick in, which signals a particularly strong sensitivity to

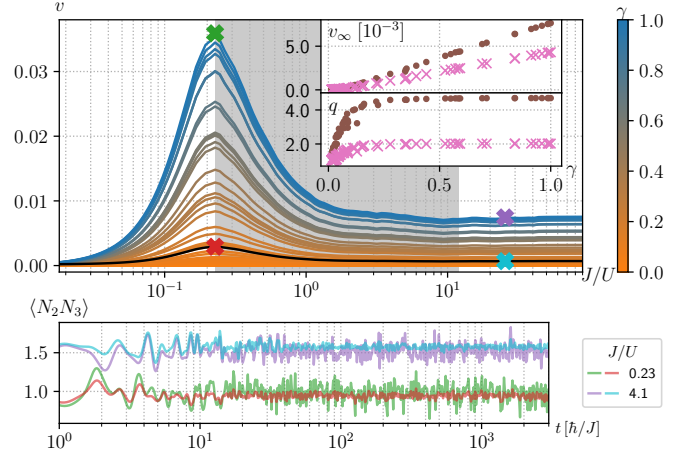


FIG. 1. Fluctuations of ($k = 2$)P observables of the Bose-Hubbard model (1), for $N = 6$ particles loaded each into one of the $L = 6$ lattice sites, and variable degrees (color bar) $\gamma \in [1/N!; 1]$ of the particles' mutual distinguishability. Top: Operator average v , Eq. (3), of the temporal variance (2) vs. J/U , with variable γ generated by 100 randomly defined internal states of the particles [63]. The black curve highlights the case analyzed in Fig. 2(d). Dots in the insets display the plateau value v_{∞} for large J/U , and the enhancement $q = v_{\text{max}}/v_{\infty}$ of the maximal fluctuations v_{max} at $J/U \simeq 0.23$, as functions of γ . Crosses indicate analogous quantities for the average $\sum_{i \neq j} \text{Var}_t[N_i N_j]/L(L-1)$ of two-point correlators. Bottom: Long-time series of $\langle N_2(t)N_3(t) \rangle$ for four combinations of J/U (legend) and γ (identified by equally colored crosses in the top panel). For visibility, the curves for $J/U = 4.1$ are shifted upwards by 0.8.

MBI at the transition to quantum chaos. We also extract q and v_{∞} for the experimentally more accessible average $\sum_{i \neq j} \text{Var}_t[N_i N_j]/L(L-1)$ over all two-point density correlations [29, 63, 65], and observe the same qualitative behavior. The long-time series of $\langle N_2(t)N_3(t) \rangle$, for four values of J/U and γ , are given in the bottom panel of Fig. 1, with strongest—MBI-induced—fluctuations for intermediate $J/U \simeq 0.23$ and $\gamma = 1$, in agreement with the above.

The amplification of v with increasing γ at the border of the chaotic domain (witnessed by q), is due to the mixing of *immanonic* [24] interference contributions to the dynamics: The bosonic symmetry of the full system, including both external and internal dof, implies that H , O and ρ (as operators on $\mathcal{H}_{\text{ext}}^{\otimes N}$) commute with particle permutations. By the Schur-Weyl duality [34, 66], these operators thus decompose into sectors labelled by the integer partitions (or Young diagrams) $\lambda = (N), (N-1, 1), (N-2, 1, 1), (N-2, 2), \dots$ of N . Each sector is characterized by a specific exchange symmetry of the particles, with (N) and $(1, 1, \dots)$ corresponding to bosonic and fermionic symmetry, respectively. The intermediate sectors describe *immanonic* [24]—neither fully symmetric nor fully anti-symmetric—exchange symmetries. Every sector further decomposes [63] into ν_{λ} identical blocks,

each of dimension d_λ , and we denote by $\{|\lambda, m\rangle\}_{m=1,\dots,d_\lambda}$ the Young basis [34, 66], built upon the Wannier basis, of one such block. Diagonalizing H in this very block, we find the eigenstates $|E_\alpha^\lambda\rangle = \sum_{m=1}^{d_\lambda} c_{\alpha m}^\lambda |\lambda, m\rangle$, with respect to which we represent the observable and the initial state, $O_{\alpha\beta}^\lambda = \langle E_\alpha^\lambda | O | E_\beta^\lambda \rangle$ and $\rho_{\alpha\beta}^\lambda = \nu_\lambda \langle E_\alpha^\lambda | \rho | E_\beta^\lambda \rangle / p_\lambda$. Here, p_λ denotes the overlap of ρ with sector λ , such that $\sum_\lambda p_\lambda = 1$. With this, $\sum_\alpha \rho_{\alpha\alpha}^\lambda = 1$, and trace and purity of ρ read $\text{tr} \rho = \sum_\lambda \sum_{\alpha=1}^{\nu_\lambda} \sum_\alpha p_\lambda \rho_{\alpha\alpha}^\lambda / \nu_\lambda = 1$ and $\gamma = \sum_\lambda p_\lambda^2 \gamma_\lambda / \nu_\lambda$, with $\gamma_\lambda = \text{tr}[(\rho^\lambda)^2]$, respectively.

The above structure allows to decompose v as given by (3) into its immanonic contributions. In the absence of degeneracies between energy levels and between energy gaps, within each block and between λ -sectors, a straightforward calculation shows [63]

$$v = \sum_\lambda p_\lambda^2 v_\lambda, \quad v_\lambda = \sum_{\alpha \neq \beta} |\rho_{\alpha\beta}^\lambda|^2 |\widehat{O_{\alpha\beta}^\lambda}|^2. \quad (4)$$

The individual contributions are determined by the squared overlaps p_λ^2 , and by the off-diagonal elements $|\rho_{\alpha\beta}^\lambda|^2$, $|\widehat{O_{\alpha\beta}^\lambda}|^2$ of initial state and observable in the eigenbasis. Figure 2(b) (upper panel) shows p_λ as a function of γ , for the same initial states as in Fig. 1. For distinguishable particles (minimal γ), the state is distributed over all sectors, with the mixed-symmetry sector $\lambda = (3, 2, 1)$ contributing most. With increasing γ , i.e., ever more indistinguishable particles, the population $p_{(N)}$ of the symmetric (*bosonic*) sector continuously increases, while the other p_λ vanish in the bosonic limit, where the fluctuations Eq. (3,4) (see lower panel of Fig. 1) are thus governed by purely bosonic MBI.

To disentangle the contributions of state and observable to v_λ in Eq. (4), we develop a statistical model for $|\rho_{\alpha\beta}^\lambda|^2$ and $|\widehat{O_{\alpha\beta}^\lambda}|^2$ in the following. Let us first look into ρ . Figure 2(a) illustrates the delocalization of the initial state seeding the fluctuations displayed in Fig. 1, in the energy eigenbasis of the largest six sectors [carrying between 68% (distinguishable particles) and 100% (indistinguishable particles) of the initial state for all γ , cf. Fig. 2(b)]. The thicker solid lines show the effective number $d_\lambda^{\text{eff}} = C_\lambda / I_\lambda$ of populated levels, quantified in terms of the inverse participation ratio $I_\lambda = \sum_\alpha |\rho_{\alpha\alpha}^\lambda|^2$. From the strongly interacting limit $J/U \rightarrow 0$, d_λ^{eff} grows with increasing tunneling strength, reaching a maximum in most sectors in the range $J/U \in [3; 4]$. Due to residual fluctuations of $\rho_{\alpha\alpha}$, $1/I_\lambda$ generically underestimates the actual number of populated eigenstates. We correct this by the multiplicative factor C_λ which enforces $d_\lambda^{\text{eff}} \rightarrow d_\lambda$ in the regime of strongest delocalization. Such strong delocalization correlates with the emergence of quantum chaos as identified by eigenstate ergodicity in the individual λ -sectors, following the analysis of Refs. [59–61] for indistinguishable bosons, and here quantified via the fractal dimension $D_1^{\lambda,\alpha} = -\sum_{m=1}^{d_\lambda} |c_{\alpha m}^\lambda|^2 \log_{d_\lambda} |c_{\alpha m}^\lambda|^2$ of the eigenstates in the Young basis. The inset of

Fig. 2(a) shows the mean value $\langle D_1^{\lambda,\alpha} \rangle$ and the variance $\text{Var}(D_1^{\lambda,\alpha})$, taken over the 60 eigenstates closest in energy to the initial state, for each λ -sector. A substantial delocalization occurs for J/U roughly between 0.23 and 11 (shaded area), where the mean values reach their maxima, accompanied by a drop of the variances by at least one order of magnitude, attesting a strongly uniform eigenstate structure in all shown sectors. Consequently, the chaotic domain identified for indistinguishable bosons [59] persists for mixed particle-exchange symmetry.

As for the observable, we assume the averaged matrix elements $|\widehat{O_{\alpha\beta}^\lambda}|^2$ in Eq. (4) to vanish outside a band of width W_λ (i.e., $|\widehat{O_{\alpha\beta}^\lambda}|^2 \rightarrow 0$, for $|\alpha - \beta| \gg W_\lambda$), at least within the chaotic domain, as stated by the eigenstate thermalization hypothesis [67–72] [73]. Figure 2(a) confirms that assumption for three exemplary values of J/U , notably with a narrow and structureless band for $J/U = 0.86$, well within the chaotic domain. We estimate the bandwidth W_λ by the standard deviations of the (normalized) probability densities $f_\beta^{(\alpha)} \propto |\widehat{O_{\alpha\beta}^\lambda}|^2$, $\beta \neq \alpha$, for each α , averaged over α . Figure 2(a) shows the resulting W_λ (dashed lines) versus J/U , in the largest six sectors.

Given the population of d_λ^{eff} eigenstates by the initial state ρ , together with the observable's bandwidth W_λ , and assuming statistical independence of the matrix elements $|\rho_{\alpha\beta}^\lambda|^2$ and $|\widehat{O_{\alpha\beta}^\lambda}|^2$, we can [63] factorize

$$v_\lambda \approx R_\lambda A_\lambda, \quad R_\lambda = \frac{\sum_{\alpha \neq \beta} |\rho_{\alpha\beta}^\lambda|^2}{\max(d_\lambda^{\text{eff}}, W_\lambda)}, \quad A_\lambda = \frac{\sum_{\alpha \neq \beta} |\widehat{O_{\alpha\beta}^\lambda}|^2}{d_\lambda}, \quad (5)$$

as qualitatively underpinned by Fig. 2(d), for a state with $\gamma = 0.15$, in the largest six sectors (which carry 99.2% of ρ for this γ value). Note that weighting those v_λ by the squares of the associated p_λ [black vertical line in Fig. 2(b)], according to Eq. (4), results in the black curve highlighted in the upper panel of Fig. 1.

To elucidate the origin of the maximum of v at the transition to quantum chaos, we further analyze the dependence of R_λ and A_λ on J/U : As shown in Fig. 2(d) (lower panel), A_λ is, to a good approximation, independent of J/U , and of order one in all contributing sectors. Consequently, the dependence of v_λ on J/U is predominantly controlled by R_λ —which encodes the competition between the coherences (in the numerator) and the delocalization of the initial state or of the observable (in the denominator), in the eigenbasis. This entails an enhanced sensitivity of v_λ on the coherences $|\rho_{\alpha\beta}^\lambda|^2$ precisely at the crossover to the chaotic domain: For $J/U \rightarrow 0$, the eigenstates approach the Young basis states. Hence, for all initial states which are sufficiently localized on a small number (of order $1/\gamma_\lambda$) of Young basis states in each sector, the numerator $\sum_{\alpha \neq \beta} |\rho_{\alpha\beta}^\lambda|^2 = \gamma_\lambda - I_\lambda$ of R_λ is substantially suppressed through increasing I_λ in this limit. States with well-defined external occu-

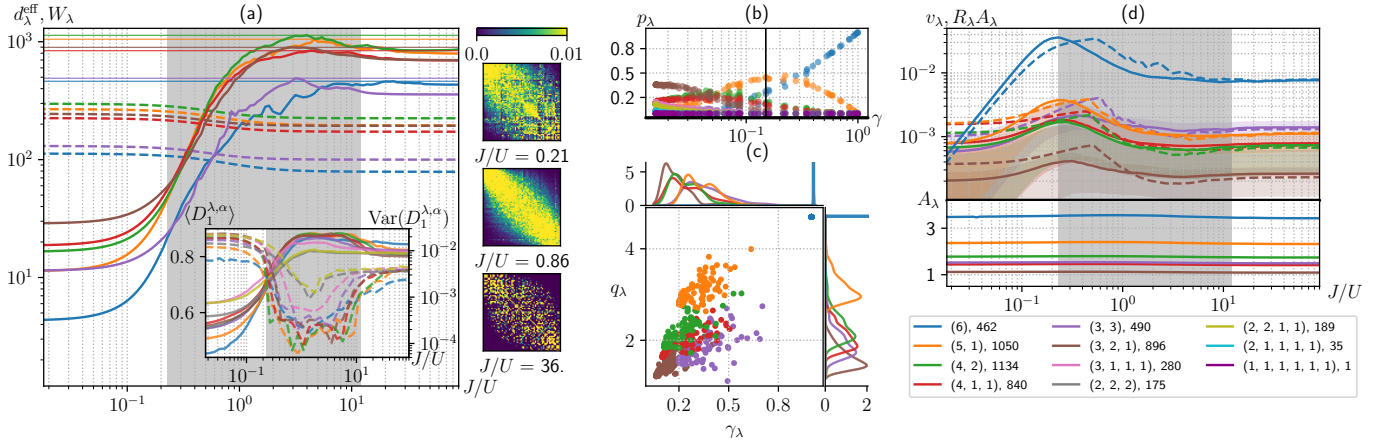


FIG. 2. Ingredients determining the averaged temporal variance of $(k=2)P$ observables shown in Fig. 1, for $N = L = 6$, as functions of J/U , and of the particles' mutual distinguishability $\gamma \in [1/N!; 1]$. (a) Delocalization of the external initial state's component ρ^λ on the symmetry sector λ in the associated eigenbasis, measured by the number d_λ^{eff} of effectively populated eigenstates (solid), and bandwidth W_λ (dashed) of the averaged observable $|\widehat{O_{\alpha\beta}^\lambda}|^2$, versus J/U , in the largest six sectors [block dimensions d_λ are marked by thin lines and given in the legend on the very right bottom (e.g. $\lambda = (6), d_\lambda = 462$)]. Inset: Average delocalization of the 60 eigenstates closest in energy to the initial state per symmetry sector λ , quantified by their mean fractal dimension $\langle D_1^{\lambda,\alpha} \rangle$ (solid) and the associated variance $\text{Var}(D_1^{\lambda,\alpha})$ (dashed) [59–61], in the respective Young basis set, for the largest nine sectors (see legend; the two remaining sectors are omitted because of their small dimensions). Panels on the right: Matrix structure (intensities indicated by the color bar) of $|\widehat{O_{\alpha\beta}^\lambda}|^2$ in the bosonic sector, for three values of J/U , to appreciate the averaged observable's band structure. (b) Sector weights p_λ versus γ , color coded according to the legend on the bottom right. The vertical black line indicates $\gamma = 0.15$. (c) Joint distribution with smoothed marginals of q_λ and γ_λ per sector, sampled by random initial states as in Fig. 1. $q_\lambda, \gamma_\lambda$ both reach their maxima in the bosonic sector. (d) Upper panel: Comparison of v_λ (solid) to the factorized approximation $R_\lambda A_\lambda$ (dashed) according to Eq. (5), versus J/U , in the first six symmetry sectors (see legend), for $\gamma \simeq 0.15$. Color shaded areas indicate the variation of v_λ for random initial states [63] with variable degree γ of distinguishability. Lower panel: Dependence of A_λ , as used in the upper panel, on J/U .

pations such as considered in Figs. 1, 2 belong to this class [63]. This is captured by the decreasing left tails of the v_λ in Fig. 2(d). Instead, for J/U within and beyond the range of fully developed quantum chaos, the initial state is strongly delocalized in the eigenbasis [recall $d_\lambda^{\text{eff}} \approx d_\lambda$ in Fig. 2(a)], resulting in a small asymptotic value $R_\lambda^\infty \approx (\gamma_\lambda - I_\lambda^\infty)/d_\lambda \ll 1$ for large J/U . At the transition between the two parameter ranges, when the eigenstates undergo the transformation from localized to ergodic, R_λ exhibits a maximum, since ρ^λ already populates a substantial energy window, resulting in an enhanced contribution by coherences, which is not yet suppressed by ergodicity ($d_\lambda^{\text{eff}} < d_\lambda$). These coherences $|\rho_{\alpha\beta}^\lambda|^2$, in turn, are mainly controlled by the purity of the state's component in the given sector.

Figure 2(c) correlates the sector-specific enhancement $q_\lambda = v_\lambda^{\text{max}}/v_\lambda^\infty$ with γ_λ , again for all contributing sectors. Both quantities exhibit their maximal values (with a non-vanishing distance to all other sectors) in the bosonic sector. For distinguishable particles ($\gamma = 1/N!$), the total fluctuations v are given by the weighted sum (4) of v_λ from all sectors, leading to $q < q_{(N)}$. The transition to indistinguishable particles ($\gamma \rightarrow 1$) is, in essence, controlled by the increasing weight $p_{(N)}^2$ of the bosonic sector, by virtue of Eq. (4), while the precise dependence of

v_λ on γ does not play a major role, since $v_{(N)}$ overwhelms all remaining v_λ by at least one order of magnitude, see Fig. 2(d). This results in $q \rightarrow q_{(N)}$, manifest in the sharp growth of q observed in the inset of Fig. 1 for $0 \lesssim \gamma \lesssim 0.2$. For $\gamma \gtrsim 0.4$, the bosonic sector is already the dominant contribution [Fig. 2(b)], as reflected by the saturation of q (with a saturation value $q \approx q_{(N)}$) [cf. Fig. 1 (inset)].

We have thus seen how many-body coherences populated by generic initial states—which spread over the many-particle eigenstates of the N -particle Bose-Hubbard model as quantum chaos kicks in—leave a statistically robust imprint in the long-time fluctuations of k -particle observables. While these fluctuations persist in the limit of fully distinguishable particles, together with the eigenstates' delocalization indicative of (interaction-induced) quantum chaos, they are significantly amplified

- (i) by many-body interference contributions stemming, in particular, from the bosonic symmetry sector with monotonically increasing weight as the particles turn more indistinguishable;
- (ii) locally in J/U , for any level of distinguishability, at the onset of chaos.

The latter reflects the enhanced sensitivity of a quantum system's particularly complex eigenstate structure (an-

chored in the underlying phase space's topological metamorphosis) at the chaos transition [10], which is inherited by single- as well as by many-particle transition amplitudes [74–76]. Therefore, only full resolution of the initially populated immanonic spectral components permits a quantitatively faithful statistical description of complex many-body quantum systems, and the discrimination of classical (i.e., interaction-induced) from truly quantum (due to many-particle interferences) causes of dynamical complexity.

The authors thank Dominik Lentrodt for fruitful discussions. The authors acknowledge support by the state of Baden-Württemberg through bwHPC and the German Research Foundation (DFG) through Grants No. INST 40/575-1 FUGG (JUSTUS 2 cluster), and No. 402552777. E.G.C. acknowledges support from the Georg H. Endress foundation. E.B., L.P. and A.R. acknowledge support by Spanish MCIN/AEI/10.13039/501100011033 through Grant No. PID2020-114830GB-I00.

eric.brunner@physik.uni-freiburg.de

[†] Current address: CESAM Research Unit, University of Liège, 4000 Liège, Belgium

- [1] B. Chirikov and V. Vecheslavov, *Astron. Astrophys.* **221**, 146 (1989).
- [2] J. Laskar and M. Gastineau, *Nature* **459**, 817 (2009).
- [3] N. Bohr, *Nature* **137**, 344 (1936).
- [4] L. Landau and E. Lifschitz, *Lehrbuch der Theoretischen Physik, Band V: Statistische Physik, Teil 1* (Akademie-Verlag, Berlin, 1984).
- [5] S. Sachdev, *Quantum Phase Transitions* (Cambridge Univ. Press, Cambridge, 2011).
- [6] M. L. Mehta, *Random Matrices*, 3rd ed. (Elsevier, Amsterdam, 1991).
- [7] E. Davies, *Quantum theory of open quantum systems* (Academic Press, New York, 1976).
- [8] R. Alicki and K. Lendi, *Quantum Dynamical Semigroups and Applications* (Springer Verlag, Berlin, 1987).
- [9] H.-P. Breuer and F. Petruccione, *The Theory of Open Quantum Systems* (Cambridge Univ. Press, Cambridge, 2002).
- [10] M. J. Giannoni, A. Voros, and J. Zinn-Justin, eds., *Les Houches Session LII: Chaos and Quantum Physics* (North-Holland, Amsterdam, 1989).
- [11] T. Guhr and H. A. Weidenmüller, *Ann. Phys.* **193**, 472 (1989).
- [12] I. Rotter, *Rep. Prog. Phys.* **54**, 635 (1991).
- [13] A. Holle, J. Main, G. Wiebusch, H. Rottke, and K. H. Welge, *Phys. Rev. Lett.* **61**, 161 (1988).
- [14] C. Iu, G. R. Welch, M. M. Kash, D. Kleppner, D. Delande, and J. C. Gay, *Phys. Rev. Lett.* **66**, 145 (1991).
- [15] A. Krug and A. Buchleitner, *Phys. Rev. Lett.* **86**, 3538 (2001).
- [16] F. Moore, J. Robinson, C. Bharucha, B. Sundaram, and M. Raizen, *Phys. Rev. Lett.* **75**, 4598 (1995).
- [17] S. Wimberger, I. Guarneri, and S. Fishman, *Phys. Rev. Lett.* **92**, 084102 (2004).
- [18] F. Meinert, M. J. Mark, E. Kirilov, K. Lauber, P. Weinmann, M. Gröbner, and H.-C. Nägerl, *Phys. Rev. Lett.* **112**, 193003 (2014).
- [19] A. M. Kaufman, M. E. Tai, A. Lukin, M. Rispoli, R. Schittko, P. M. Preiss, and M. Greiner, *Science* **353**, 794 (2016).
- [20] H. Liu and S. Vardhan, *J. High Energ. Phys.* **2021** (3), 88.
- [21] R. Garbaczewski and R. Olkiewicz, eds., *Dynamics of Dissipation* (Springer Verlag, Berlin, 2002).
- [22] J. v. Milczewski, G. Diercksen, and T. Uzer, *Phys. Rev. Lett.* **76**, 2890 (1996).
- [23] L. Landau and E. Lifschitz, *Lehrbuch der Theoretischen Physik, Band III: Quantenmechanik* (Akademie-Verlag, Berlin, 1985).
- [24] M. C. Tichy and K. Mølmer, *Phys. Rev. A* **96**, 022119 (2017).
- [25] C. K. Hong, Z. Y. Ou, and L. Mandel, *Phys. Rev. Lett.* **59**, 2044 (1987).
- [26] M. C. Tichy, M. Tiersch, F. de Melo, F. Mintert, and A. Buchleitner, *Phys. Rev. Lett.* **104**, 220405 (2010).
- [27] G. Dufour, T. Brünner, C. Dittel, G. Weihs, R. Keil, and A. Buchleitner, *New J. Phys.* **19**, 125015 (2017).
- [28] V. S. Shchesnovich and M. E. O. Bezerra, *Phys. Rev. A* **98**, 033805 (2018).
- [29] T. Giordani, F. Flamini, M. Pompili, N. Viggianiello, N. Spagnolo, A. Crespi, R. Osellame, N. Wiebe, M. Walschaers, A. Buchleitner, and F. Sciarrino, *Nat. Phot.* **12**, 173 (2018).
- [30] C. Dittel, G. Dufour, M. Walschaers, G. Weihs, A. Buchleitner, and R. Keil, *Phys. Rev. Lett.* **120**, 240404 (2018).
- [31] C. Dittel, G. Dufour, M. Walschaers, G. Weihs, A. Buchleitner, and R. Keil, *Phys. Rev. A* **97**, 062116 (2018).
- [32] T. Brünner, G. Dufour, A. Rodríguez, and A. Buchleitner, *Phys. Rev. Lett.* **120**, 210401 (2018).
- [33] A. E. Jones, A. J. Menssen, H. M. Chrzanowski, T. A. Wolterink, V. S. Shchesnovich, and I. A. Walmsley, *Phys. Rev. Lett.* **125**, 123603 (2020).
- [34] G. Dufour, T. Brünner, A. Rodríguez, and A. Buchleitner, *New J. Phys.* **22**, 103006 (2020).
- [35] C. Dittel, G. Dufour, G. Weihs, and A. Buchleitner, *Phys. Rev. X* **11**, 031041 (2021).
- [36] E. Brunner, A. Buchleitner, and G. Dufour, [arXiv:2107.01686 \[cond-mat, physics:quant-ph\]](https://arxiv.org/abs/2107.01686) (2021).
- [37] M. C. Tichy, J. F. Sherson, and K. Mølmer, *Phys. Rev. A* **86**, 063630 (2012).
- [38] S. Stanisic and P. S. Turner, *Phys. Rev. A* **98**, 043839 (2018).
- [39] M. Greiner, O. Mandel, T. Esslinger, T. W. Hänsch, and I. Bloch, *Nature* **415**, 39 (2002).
- [40] I. Bloch, J. Dalibard, and W. Zwerger, *Rev. Mod. Phys.* **80**, 885 (2008).
- [41] T. Gericke, P. Würtz, D. Reitz, T. Langen, and H. Ott, *Nat. Phys.* **4**, 949 (2008).
- [42] N. Gemelke, X. Zhang, C.-L. Hung, and C. Chin, *Nature* **460**, 995 (2009).
- [43] M. Karski, L. Förster, J. M. Choi, W. Alt, A. Widera, and D. Meschede, *Phys. Rev. Lett.* **102**, 053001 (2009).
- [44] W. S. Bakr, A. Peng, M. E. Tai, R. Ma, J. Simon, J. I. Gillen, S. Folling, L. Pollet, and M. Greiner, *Science* **329**, 547 (2010).
- [45] J. F. Sherson, C. Weitenberg, M. Endres, M. Cheneau, I. Bloch, and S. Kuhr, *Nature* **467**, 68 (2010).
- [46] A. Lukin, M. Rispoli, R. Schittko, M. E. Tai, A. M. Kaufman, S. Choi, V. Khemani, J. Léonard, and M. Greiner,

- Science **364**, 256 (2019).
- [47] M. Rispoli, A. Lukin, R. Schittko, S. Kim, M. E. Tai, J. Léonard, and M. Greiner, *Nature* **573**, 385 (2019).
 - [48] O. Giraud, N. Macé, É. Vernier, and F. Alet, *Phys. Rev. X* **12**, 011006 (2022).
 - [49] M. P. A. Fisher, P. B. Weichman, G. Grinstein, and D. S. Fisher, *Phys. Rev. B* **40**, 546 (1989).
 - [50] M. Lewenstein, A. Sanpera, V. Ahufinger, B. Damski, A. Sen(De), and U. Sen, *Adv. Phys.* **56**, 243 (2007).
 - [51] M. A. Cazalilla, R. Citro, T. Giamarchi, E. Orignac, and M. Rigol, *Rev. Mod. Phys.* **83**, 1405 (2011).
 - [52] K. V. Krutitsky, *Phys. Rep.* **607**, 1 (2016).
 - [53] A. Buchleitner and A. R. Kolovsky, *Phys. Rev. Lett.* **91**, 253002 (2003).
 - [54] A. R. Kolovsky and A. Buchleitner, *Europhys. Lett.* **68**, 632 (2004).
 - [55] C. Kollath, G. Roux, G. Biroli, and A. M. Läuchli, *J. Stat. Mech.* **2010**, P08011 (2010).
 - [56] W. Beugeling, A. Andreanov, and M. Haque, *J. Stat. Mech.* **2015**, P02002 (2015).
 - [57] R. Dubertrand and S. Müller, *New J. Phys.* **18**, 033009 (2016).
 - [58] W. Beugeling, A. Bäcker, R. Moessner, and M. Haque, *Phys. Rev. E* **98**, 022204 (2018).
 - [59] L. Pausch, E. G. Carnio, A. Rodríguez, and A. Buchleitner, *Phys. Rev. Lett.* **126**, 150601 (2021).
 - [60] L. Pausch, E. G. Carnio, A. Buchleitner, and A. Rodríguez, *New J. Phys.* **23**, 123036 (2021).
 - [61] L. Pausch, A. Buchleitner, E. G. Carnio, and A. Rodríguez, *J. Phys. A* **55**, 324002 (2022).
 - [62] E. Brunner, *Many-body interference, partial distinguishability and entanglement* (2019), M.Sc. Thesis, Albert-Ludwigs-Universität Freiburg.
 - [63] See Supplemental Material at [URL will be inserted by publisher] for further details.
 - [64] Note that v is independent of the chosen operator basis.
 - [65] M. Walschaers, J. Kuipers, J.-D. Urbina, K. Mayer, M. C. Tichy, K. Richter, and A. Buchleitner, *New J. Phys.* **18**, 032001 (2016).
 - [66] W. Fulton and J. Harris, *Representation Theory* (Springer, New York, 2004).
 - [67] M. Feingold and A. Peres, *Phys. Rev. A* **34**, 591 (1986).
 - [68] J. M. Deutsch, *Phys. Rev. A* **43**, 2046 (1991).
 - [69] M. Srednicki, *Phys. Rev. E* **50**, 888 (1994).
 - [70] M. Srednicki, *J. Phys. A* **32**, 1163 (1999).
 - [71] M. Hiller, T. Kottos, and T. Geisel, *Phys. Rev. A* **73**, 061604 (2006).
 - [72] J. M. Deutsch, *Rep. Prog. Phys.* **81**, 082001 (2018).
 - [73] Note that $|\widehat{O_{\alpha\beta}^\lambda}|^2 \propto \text{tr}_{N-k}[\varepsilon_\alpha^{\lambda, N-k} \varepsilon_\beta^{\lambda, N-k}]$, with $\varepsilon_\alpha^{\lambda, N-k} = \text{tr}_k[|E_\alpha^\lambda\rangle\langle E_\alpha^\lambda|]$ the reduced $(N-k)$ P eigenstates [63], i.e., a banded structure of $|\widehat{O_{\alpha\beta}^\lambda}|^2$ implies a rapid transition from almost parallel to almost orthogonal (with respect to the Hilbert-Schmidt inner product) reduced eigenstates $\varepsilon_\alpha^{\lambda, N-k}$, with increasing $|\alpha - \beta|$. A loss of eigenstate orthogonality upon tracing over a k P subset implies entanglement between that subset and the remainder.
 - [74] J. M. Robbins, *Phys. Rev. A* **40**, 2128 (1989).
 - [75] T. H. Seligman and H. A. Weidenmüller, *J. Phys. A* **27**, 7915 (1994).
 - [76] P. Schlagheck, D. Ullmo, J. D. Urbina, K. Richter, and S. Tomsovic, *Phys. Rev. Lett.* **123**, 215302 (2019).

Supplemental Material

Many-body interference at the onset of chaos

Distribution of internal states

For the numerical simulations shown in Figs. 1 and 2, we need to generate random internal states for each particle so as to cover the transition from distinguishable to indistinguishable particles, quantified in terms of the purity $\gamma = \text{tr} \rho^2$ of the reduced external state ρ , as uniformly as possible. The straightforward ansatz to generate random initial states, e.g., distributed according to the Haar measure on \mathcal{H}_{int} , likely generates rather orthogonal states $|\phi_i\rangle$ for the particles and, thus, only samples the region of small γ . To circumvent this problem, we employ the same two-step sampling procedure as used in [36]: We generate random pure internal states $|\phi_i\rangle = \sum_\sigma \phi_{i\sigma} |\sigma\rangle$ for the particle in mode i , where the states $|\sigma\rangle$ form a basis of \mathcal{H}_{int} (the dimension of the internal Hilbert space has to be larger than or equal to the number of particles). To cover the vicinity of indistinguishable particles, we initialize a unit vector $|e\rangle \in \mathcal{H}_{\text{int}}$ and perturb it by a small $|g_i\rangle$, with normally distributed real and imaginary parts of the components of $|g_i\rangle$, with zero mean and variance ε . For sufficiently small ε , the resulting states

$|\phi_i\rangle = |e\rangle + |g_i\rangle$, after renormalization, are almost parallel. As ε becomes larger, the relative contribution of the constant vector $|e\rangle$ becomes negligible and we sample the unit sphere in \mathcal{H}_{int} uniformly in the limit $\varepsilon \gg 1$. In the second step, we employ a similar procedure in the neighborhood of distinguishable particles. For this we choose for each particle i an orthogonal unit vector $|e_i\rangle \in \mathcal{H}_{\text{int}}$ and, again, add a perturbation $|g_i\rangle$ with normally distributed components in \mathbb{C} , with zero mean and variance ε , followed by renormalization. For large ε , the contribution from $|e_i\rangle$ to $|\phi_i\rangle = |e_i\rangle + |g_i\rangle$ can be neglected, leading to uniform sampling of the unit sphere in \mathcal{H}_{int} . As ε becomes small, $\varepsilon \ll 1$, we sample states $|\phi_i\rangle$ close to perfectly distinguishable particles.

Density correlation mean

The operator average over a basis of k P observables yields a statistically robust estimate of experimentally accessible k -point correlation measurements of the external modes. To show this for the case $k = 2$, we replace

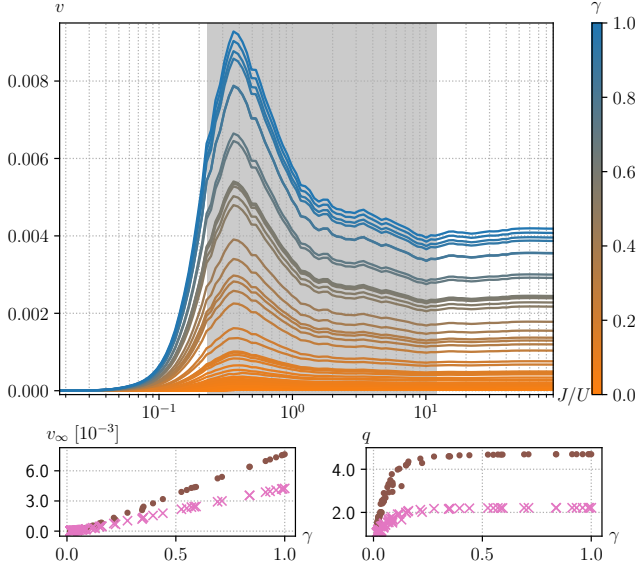


FIG. S1. Infinite time variance v [cf. Eq.(2)] as a function of J/U for 100 random initial states of varying partial distinguishability, as quantified by the purity γ (color bar), for the average over all two-point density correlations (text). The lower panel shows the plateau value v_∞ and the relative peak-height q as functions of γ .

the average in Eq. (3) by an average over all two-point density correlations

$$v = \frac{1}{L(L-1)} \sum_{i \neq j} \text{Var}_t[N_i N_j], \quad (\text{S1})$$

where the operator $N_i = \sum_{\sigma=1}^s a_{i\sigma}^\dagger a_{i\sigma}$ counts the number of particles on site i , irrespective of their internal states. Figure S1 shows v for this average as a function of J/U and of the particles' indistinguishability, quantified by $\gamma = \text{tr} \rho^2$ (as in Fig. 1). We observe the same behavior as for the operator average, Eq (3). The average v (S1) shows a peak for $J/U \approx 0.35$ (note a small shift to larger J/U values in comparison to the operator average) followed by a decline to a plateau value v_∞ . The dependence of v_∞ and of the relative peak height $q = v_{\text{max}}/v_\infty$ on γ is shown in the lower panels of Fig. S1 [cf. the insets of Fig. 1(a)]. We observe, up to a constant scaling, exactly the same strictly monotonic increase of both quantities with γ as for the average of Eq. (3). Note that to resolve this constant scaling factor between both averages, one needs to divide Eq. (3) by the dimensionality of the space of external two-particle observables. We omit this rather technical aspect here, since it is not of importance for our discussion.

Schur-Weyl duality

Since dynamics and measurements are restricted to the external dof only, we trace out the internal dof. The reduced external system is conveniently described by the N th tensor power of the external single-particle Hilbert space, $\mathcal{H}_{\text{ext}}^{\otimes N}$. On this space, the symmetric and the unitary groups, S_N and $U(L)$, act according to $\pi |m_1, \dots, m_N\rangle := |m_{\pi^{-1}(1)}, \dots, m_{\pi^{-1}(N)}\rangle$, $\pi \in S_N$, and $U |m_1, \dots, m_N\rangle := U |m_1\rangle \otimes \dots \otimes U |m_N\rangle$, $U \in U(L)$, respectively. Schur-Weyl duality states that these two group actions are dual to each other [66]. This implies that the external N -particle space decomposes into a direct sum of irreducible representations of S_N and $U(L)$, $\mathcal{H}_{S_N}^\lambda$ and $\mathcal{H}_{U(L)}^\lambda$, i.e.,

$$\mathcal{H}_{\text{ext}}^{\otimes N} = \bigoplus_{\lambda} \left(\mathcal{H}_{S_N}^\lambda \otimes \mathcal{H}_{U(L)}^\lambda \right). \quad (\text{S2})$$

The direct sum runs over Young diagrams (i.e., integer partitions of N), such as $\lambda = (N), (N-1, 1), (N-2, 1, 1), (N-2, 2), \dots, (1, \dots, 1)$. While the reduced states of perfectly indistinguishable bosons only occupy the symmetric sector (which we call the *bosonic* sector), $\lambda = (N)$, the reduced states of partially distinguishable particles typically occupy all sectors, as detailed in the main text.

Equation (S2) provides a convenient basis $|\lambda, i, m\rangle = |\lambda, i\rangle \otimes |\lambda, m\rangle$ of $\mathcal{H}_{\text{ext}}^{\otimes N}$, where i and m index basis states of the irreducible representations $\mathcal{H}_{S_N}^\lambda$ and $\mathcal{H}_{U(L)}^\lambda$, respectively. Each such basis state of $\mathcal{H}_{S_N}^\lambda$ and $\mathcal{H}_{U(L)}^\lambda$ corresponds to a standard, respectively semi-standard Young tableau of shape λ [34, 66]. The number of standard and semi-standard Young tableaux, ν_λ and d_λ , are combinatorial in nature and can be calculated via hook length formulas [66]. The table below lists them for the considered case of $N = L = 6$.

λ	ν_λ	d_λ
(6)	1	462
(5, 1)	5	1050
(4, 2)	9	1134
(4, 1, 1)	10	840
(3, 3)	5	490
(3, 2, 1)	16	896
(3, 1, 1, 1)	10	280
(2, 2, 2)	5	175
(2, 2, 1, 1)	9	189
(2, 1, 1, 1, 1)	5	35
(1, 1, 1, 1, 1, 1)	1	1

Adding up the dimensions with their corresponding multiplicities leads to the total dimension $\sum_{\lambda} \nu_\lambda d_\lambda = L^N = 46656$ for the considered system. Note that the dynamics of the system is exclusively described by the irreducible

representations of the unitary group, $\mathcal{H}_{U(L)}^\lambda$. Hence, the numbers ν_λ of basis states $|\lambda, i\rangle$ of the irreducible representations of the symmetric group constitutes merely a multiplicity factor, and each symmetry sector λ decomposes into ν_λ identical blocks $\mathcal{H}_{U(L)}^\lambda$ of dimension d_λ . Since all blocks of one sector yield identical contributions to the dynamics, we can restrict the discussion to one of them for each sector, as done in Eq. (4).

An initial state with well-defined external occupation numbers N_i occupies all Young basis states $|\lambda, m\rangle$ corresponding to semi-standard Young tableaux of shape λ compatible with the given occupation numbers. More precisely, these are exactly those Young tableaux that can be obtained by filling N_i symbols ' i ' (for $i = 1, \dots, L$) into the diagram λ by following the rules that each column must be strictly increasing and each row must be non-decreasing. The number of such tableaux for given occupation numbers $\{N_i\}$ is given by the so called Kostka-number $\kappa_\lambda(\{N_i\})$ [66]. In case of the homogeneous initial state ($N_i = 1, i = 1, \dots, L$) considered in Fig. 1 and 2, semi-standard and standard Young diagrams are actually identical, leading to $\kappa_\lambda = \nu_\lambda$. In the limit $J/U \rightarrow 0$, where the energy eigenstates approach the Young basis states, maximal localization is achieved with maximal $I_\lambda = \sum_\alpha |\rho_{\alpha\alpha}^\lambda|^2$, taking on a value larger than the inverse number of occupied Young basis states $I_\lambda \geq 1/\kappa_\lambda$ (the populations on the occupied Young basis states are typically not uniform). This localization on a small number $\kappa_\lambda \sim 1$ of energy states for $J/U \rightarrow 0$, leads to a significant suppression of the numerator $\gamma_\lambda - I_\lambda$ of R_λ [cf. Eq. (5)] in this limit. Note, moreover, that a lower tight bound of the purity γ_λ for each sector is given by $1/\kappa_\lambda$, which is achieved for perfectly distinguishable particles. Since $\kappa_{(N)} = 1$, this implies maximal purity $\gamma_{(N)} = 1$ in the bosonic sector, independent of the particles' distinguishability.

Derivation of Eq. (4)

Under the assumption of a non-degenerate spectrum, the infinite time average of the time dependent expectation is given by

$$\overline{\langle O(t) \rangle} = \sum_{\lambda, \alpha, \beta} p_\lambda \rho_{\alpha\beta}^\lambda O_{\beta\alpha}^\lambda \overline{e^{it(E_\alpha^\lambda - E_\beta^\lambda)}} = \sum_{\lambda, \alpha} p_\lambda \rho_{\alpha\alpha}^\lambda O_{\alpha\alpha}^\lambda, \quad (\text{S3})$$

with $\overline{\dots}$ indicating the integration $1/T \int_0^T dt \dots$ for $T \rightarrow \infty$. Definitions of $\rho_{\alpha\beta}^\lambda, O_{\alpha\beta}^\lambda$ are given in the main text. Integration over the appearing exponential functions yields $\delta_{\alpha\beta}$. The variance of the time signal $\langle O(t) \rangle$ is given by

$$\overline{\langle O(t) \rangle^2} = \sum_{\substack{\lambda, \alpha, \beta \\ \tau, \gamma, \delta}} p_\lambda p_\tau \rho_{\alpha\beta}^\lambda O_{\beta\alpha}^\lambda \rho_{\gamma\delta}^\tau O_{\delta\gamma}^\tau \overline{e^{it(E_\alpha^\lambda - E_\beta^\lambda)} e^{it(E_\gamma^\tau - E_\delta^\tau)}}. \quad (\text{S4})$$

Assuming no degeneracies of levels and no gap-degeneracies between and within the λ -sectors, the time integration either decouples the sums over λ and τ or enforces a $\delta_{\lambda\tau}$, leading to

$$\overline{\langle O(t) \rangle^2} = \sum_{\lambda, \alpha, \tau, \gamma} p_\lambda p_\tau \rho_{\alpha\alpha}^\lambda O_{\alpha\alpha}^\lambda \rho_{\gamma\gamma}^\tau O_{\gamma\gamma}^\tau + \sum_{\lambda, \alpha \neq \beta} p_\lambda^2 |\rho_{\alpha\beta}^\lambda|^2 |O_{\alpha\beta}^\lambda|^2. \quad (\text{S5})$$

The first term is equal to the square of the time-averaged expectation $\overline{\langle O(t) \rangle}^2$, Eq. (S3). Subtracting this yields the variance

$$\text{Var}_t[O] = \sum_{\lambda, \alpha \neq \beta} p_\lambda^2 |\rho_{\alpha\beta}^\lambda|^2 |O_{\alpha\beta}^\lambda|^2. \quad (\text{S6})$$

Note that the variance is linear in $|O_{\alpha\beta}^\lambda|^2$, such that we can take the operator average over observables into the sum

$$\widehat{\text{Var}_t[O]} = \sum_{\lambda, \alpha \neq \beta} p_\lambda^2 |\rho_{\alpha\beta}^\lambda|^2 \widehat{|O_{\alpha\beta}^\lambda|^2}, \quad (\text{S7})$$

which is Eq. (4).

Derivation of Eq. (5)

We show the factorization of ν_λ into $R_\lambda A_\lambda$ according to Eq. (4), under the considered statistical assumptions on the matrix elements $|\rho_{\alpha\beta}^\lambda|^2$ and $|O_{\alpha\beta}^\lambda|^2$, namely that ρ^λ effectively occupies d_λ^{eff} energy levels, that the observable is banded with bandwidth W_λ , and that the matrix elements of state and observable are statistically independent. For convenience, we define δ_α^ρ to be 1 on the d_λ^{eff} eigenstates (indexed by α) closest in energy to the energy expectation of the considered homogeneous initial state, $E = \text{tr}[\rho H] = 0$, and 0 elsewhere. Moreover let $\delta_{\alpha\beta}^O$ be 1 for $|\alpha - \beta| \leq W_\lambda$ and 0 for $|\alpha - \beta| > W_\lambda$. With this we can calculate

$$\begin{aligned} \sum_{\alpha \neq \beta} |\rho_{\alpha\beta}^\lambda|^2 |O_{\alpha\beta}^\lambda|^2 &= \sum_{\alpha \neq \beta} |\rho_{\alpha\beta}^\lambda|^2 |O_{\alpha\beta}^\lambda|^2 \delta_\alpha^\rho \delta_\beta^\rho \delta_{\alpha\beta}^O \\ &= \frac{1}{\mathcal{N}} \sum_{\alpha \neq \beta} |\rho_{\alpha\beta}^\lambda|^2 \delta_\alpha^\rho \delta_\beta^\rho \delta_{\alpha\beta}^O \sum_{\alpha' \neq \beta'} |O_{\alpha'\beta'}^\lambda|^2 \delta_{\alpha'}^\rho \delta_{\beta'}^\rho \delta_{\alpha'\beta'}^O \\ &= \frac{1}{\mathcal{N}} \frac{\mathcal{N}}{(d_\lambda^{\text{eff}})^2} \sum_{\alpha \neq \beta} |\rho_{\alpha\beta}^\lambda|^2 \delta_\alpha^\rho \delta_\beta^\rho \frac{\mathcal{N}}{d_\lambda W_\lambda} \sum_{\alpha' \neq \beta'} |O_{\alpha'\beta'}^\lambda|^2 \delta_{\alpha'}^\rho \delta_{\beta'}^\rho \delta_{\alpha'\beta'}^O \\ &= \frac{\min(d_\lambda^{\text{eff}}, W_\lambda)}{d_\lambda d_\lambda^{\text{eff}} W_\lambda} \sum_{\alpha \neq \beta} |\rho_{\alpha\beta}^\lambda|^2 \sum_{\alpha' \neq \beta'} |O_{\alpha'\beta'}^\lambda|^2 \\ &= \frac{1}{d_\lambda \max(d_\lambda^{\text{eff}}, W_\lambda)} \sum_{\alpha \neq \beta} |\rho_{\alpha\beta}^\lambda|^2 \sum_{\alpha' \neq \beta'} |O_{\alpha'\beta'}^\lambda|^2, \end{aligned}$$

with $\mathcal{N} = d_\lambda^{\text{eff}} \min(d_\lambda^{\text{eff}}, W_\lambda)$. The second equality exploits the statistical independence of the matrix elements

of state and observable. The sums in line two run over a subset of indices $\alpha \neq \beta$ of size \mathcal{N} . The sums in line three run over $(d_\lambda^{\text{eff}})^2$ and $d_\lambda W_\lambda$ indices, respectively. For this we correct by the introduced fractions in line three.

Calculation of the averaged matrix elements $\widehat{|O_{\alpha\beta}^\lambda|^2}$ of the observable

Here we derive the expression of $\widehat{|O_{\alpha\beta}^\lambda|^2}$ in terms of the Hilbert-Schmidt inner products of particle-reduced energy eigenstates, used in footnote [73] of the main text. The N th tensor power of $\mathcal{H}_{\text{ext}}^{\otimes N}$ allows for a bipartition $\mathcal{H}_{\text{ext}}^{\otimes N} = \mathcal{H}_{\text{ext}}^{\otimes k} \otimes \mathcal{H}_{\text{ext}}^{\otimes (N-k)}$ into the reduced k P space and the rest of the system. Let $\{O_i^{(k)}\}_{i=1}^{d_{\text{OP}}}$ be an orthonormal basis of the operator space of Hermitian k P operators which, together with the Hilbert-Schmidt inner product, forms a finite-dimensional Hilbert space of dimension d_{OP} . For pairs of eigenstates $|E_\alpha\rangle$ we define reduced operators $\varepsilon_{\alpha\beta}^{(k)} = \text{tr}_{(N-k)}[|E_\alpha\rangle\langle E_\beta|]$, which for $\alpha = \beta$ are just the k P reduced density operators of the eigenstate [62]. For brevity we set $A = (k), B = (N - k)$ and calcu-

late

$$\begin{aligned} \widehat{|O_{\alpha\beta}|^2} &= \sum_{i=1}^{d_{\text{OP}}} \text{tr}[O_i^A |E_\beta\rangle\langle E_\alpha|] \text{tr}[O_i^A |E_\alpha\rangle\langle E_\beta|] \\ &= \binom{N}{k}^2 \sum_{i=1}^{d_{\text{OP}}} \text{tr}_A[O_i^A \varepsilon_{\beta\alpha}^A] \text{tr}_A[O_i^A \varepsilon_{\alpha\beta}^A] \\ &= \binom{N}{k}^2 \text{tr}_A[\varepsilon_{\beta\alpha}^A \varepsilon_{\alpha\beta}^A] = \binom{N}{k}^2 \text{tr}_B[\varepsilon_{\alpha\alpha}^B \varepsilon_{\beta\beta}^B], \end{aligned}$$

where the third equality uses the fact that the $O_i^{(k)}$ are an orthonormal basis. The proportionality factor $\binom{N}{k}$ accounts for the fact that the (implicit) extension of $O_i^{(k)}$ to the full NP space $\mathcal{H}_{\text{ext}}^{\otimes N}$ is not normalized, more precisely $\text{tr}[O_i^A |E_\beta\rangle\langle E_\alpha|] = \binom{N}{k} \text{tr}_A[O_i^A \varepsilon_{\beta\alpha}^A]$ [62]. The last equality can be shown using the Schmidt decomposition $|E_\alpha\rangle = \sum_i c_i^\alpha |\phi_i^A, \phi_i^B\rangle$, which allows us to calculate

$$\begin{aligned} &\text{tr}_A[\varepsilon_{\beta\alpha}^A \varepsilon_{\alpha\beta}^A] \\ &= \text{tr}_A \left[\text{tr}_B \left[\sum_{ij} c_i^\beta c_j^\alpha |\phi_i^A \phi_j^B\rangle\langle \phi_j^A, \phi_i^B| \right] \right. \\ &\quad \times \left. \text{tr}_B \left[\sum_{k\ell} c_k^\alpha c_\ell^\beta |\phi_k^A \phi_\ell^B\rangle\langle \phi_\ell^A, \phi_k^B| \right] \right] \\ &= \sum_{ijkl} c_i^\beta c_j^\alpha c_k^\alpha c_\ell^\beta \text{tr}_A \left[\text{tr}_B \left[|\phi_i^A \phi_j^B\rangle\langle \phi_j^A, \phi_i^B| \right] \right. \\ &\quad \times \left. \text{tr}_B \left[|\phi_k^A \phi_\ell^B\rangle\langle \phi_\ell^A, \phi_k^B| \right] \right] \\ &= \sum_{ijkl} c_i^\beta c_j^\alpha c_k^\alpha c_\ell^\beta \langle \phi_j^B | \phi_i^B \rangle \langle \phi_\ell^B | \phi_k^B \rangle \langle \phi_j^A | \phi_k^A \rangle \langle \phi_\ell^A | \phi_i^A \rangle \\ &= \text{tr}_B[\varepsilon_{\alpha\alpha}^B \varepsilon_{\beta\beta}^B]. \end{aligned}$$